

# Diagnostic Performance of Multiparametric MR Imaging at 3.0 Tesla in Discriminating Prostate Cancer from Prostatitis: A Histopathologic Correlation

Elif Peker<sup>1</sup> , Didem Yasemin Sonmez<sup>1</sup> , Habip Eser Akkaya<sup>1</sup> , Serhat Hayme<sup>2</sup> , Memet Ilhan Erden<sup>1</sup> ,  
Ayse Erden<sup>1</sup> 



**Cite this article as:** Peker E, Sonmez DY, Akkaya HE, Hayme S, Erden MI, Erden A. Diagnostic Performance of Multiparametric MR Imaging at 3.0 Tesla in Discriminating Prostate Cancer from Prostatitis: A Histopathologic Correlation. *Eurasian J Med* 2018; 50: DOI 10.5152/eurasianjmed.2018.18195.

**ORCID IDs of the authors:**  
E.P. 0000-0003-3585-6848  
D.Y.S. 0000-0001-9598-6789  
H.E.A. 0000-0002-8447-3627  
S.H. 0000-0001-9428-3002  
M.I.E. 0000-0002-6274-3841  
A.E. 0000-0002-9518-5428

<sup>1</sup>Department of Radiology, Ankara University School of Medicine, Ankara, Turkey

<sup>2</sup>Department of Biostatistics, Ankara University School of Medicine, Ankara, Turkey

Received: May 18, 2018  
Accepted: August 9, 2018  
Available Online Date: November 30, 2018

Correspondence to: Elif Peker  
E-mail: elifzyurek0@yahoo.com

DOI 10.5152/eurasianjmed.2018.18195

©Copyright 2018 by the Atatürk University School of Medicine - Available online at [www.eurasianjmed.com](http://www.eurasianjmed.com)

## ABSTRACT

**Objective:** To investigate the diagnostic performance of multiparametric magnetic resonance imaging (mpMRI) in differentiating prostate cancer (PCa) from prostatitis foci.

**Materials and Methods:** This retrospective analysis included 81 biopsy-proven lesions (44 prostatitis and 37 PCa). Normalized T2-signal intensity (nT2SI) and SI on diffusion-weighted imaging (b=1000 and 2000 mm<sup>2</sup>/s), apparent diffusion coefficient (ADC) values, peak SI, SI at the end of the dynamic curves, mean peak time, mean enhancement percentage, and washout percentage obtained from dynamic contrast-enhanced imaging (DCEI) were measured.

**Results:** nT2SI (3.8 vs. 3.2, p=0.003) and ADC values (0.685×10<sup>-3</sup> mm<sup>2</sup>/s vs. 0.874×10<sup>-3</sup> mm<sup>2</sup>/s, p<0.001) were significantly higher in the prostatitis group than in the PCa group. The washout percentage was the only DCEI parameter that was significantly different between the two groups (12% vs. 4%, respectively, p=0.003). The ADC values alone showed higher sensitivity (80.5%) and specificity (75%) than all of the single criteria and most of the combined criteria. The combination of nT2SI, ADC values, and washout percentage (at least two positive criteria were sufficient for a diagnosis of PCa) yielded the highest sensitivity (77.7%) and specificity (85.7%) among all combinations.

**Conclusion:** PCa and prostatitis can be discriminated using mpMRI with high sensitivity and specificity.

**Keywords:** Prostate, prostate cancer, prostatitis, multiparametric magnetic resonance imaging, diffusion magnetic resonance imaging, T2-weighted imaging

## Introduction

Prostatitis is caused by infiltration of the prostate tissue by immune mediators. Although most cases of prostatitis are not detected due to the subclinical course, similar to prostate cancer (PCa), prostatitis is a common disease, with a prevalence ranging from 2.2% to 9.7% [1]. Bacterial prostatitis is easy to identify, whereas non-bacterial prostatitis is a diagnostic challenge for urologists [2]. Similar to PCa, prostatitis exhibits an increase in serum prostate-specific antigen (PSA) levels and benign hyperplasia [3]. For this reason, it is difficult for urologists to distinguish PCa from benign pathologies with PSA. Owing to the lack of specific laboratory tests for the diagnosis of prostatitis, radiological imaging is the most commonly used diagnostic method.

Tissue changes that are hypointense on T2-weighted imaging (T2WI) may cause difficulties in diagnosing PCa. In addition to PCa, other possible causes of hypointensity on T2WI include prostatitis, hemorrhage, scarring, and atrophy, as well as the effects of various therapies [2, 4, 5].

Given these possibilities, radiologists must make difficult decisions. Among the diagnostic alternatives, prostatitis is the most problematic condition due to the clinical and magnetic resonance (MR)-based similarities between it and PCa. Certain findings, such as wedge-shaped areas that show early contrast enhancement, absence of mass effect, and preservation of capsular integrity, are important to distinguish prostatitis from PCa [2, 4, 5]; however, in routine practice, the distinction of these two diseases is not always possible. Thus, a biopsy, which is critical, is needed for a definitive diagnosis, and its results will affect treatment options. However, technical developments in the imaging arena have introduced the possibility of a non-invasive diagnosis.

Multiparametric MR imaging (mpMRI) has been developed because the diverse information obtained from a single MR sequence cannot adequately detect and characterize PCa alone. Examination of the prostate gland with mpMRI emerged approximately 10 years ago [6].

**Table 1.** Tesla pulse sequence parameters for prostate MR

Parameter	T2W TSE	T2W TSE (HR)	T2W TSE (HR)	T1W FS CE TSE	DCEI (VIBE-FS)	DWI* EPI
Matrix size	320×310	320×310	320×310	256×192	256×205	160×102
Slice thickness (mm)	3	3.0	3.0	3	3.6	3.6
Distance factor	20%	20%	20%	20%	20%	0
Repetition time (ms)	4000	4000	4000	700	5.56	8000
Echo time (ms)	101	101	101	11	1.98	93
Echo trains per slice	9	10	13	128		N/A
Flip angle (°)	150	150	150	150	15	N/A
Acceleration factor	2	2	2	2	OFF	2
Averages	3	3	2	1	1	4
FOV (mm)	200×200	200×200	200×200	200×200	200×200	260×221
Orientation	Sagittal	Oblique axial	Oblique coronal	Oblique axial	Oblique axial	Oblique axial
Bandwidth (Hz/Px)	200	200	200	178	260	1158
Acquisition time (min:s)	4:10	4:10	3:38	3:02	4:10	4:10

T2W: T2-weighted; T1W: T1-weighted; TSE: turbo spin-echo; FOV: field of view; HR: high-resolution; FS: fat-suppressed; DCEI: dynamic contrast-enhanced imaging; DWI: diffusion-weighted imaging; EPI: echo-planar imaging; N/A: not applicable; VIBE: volumetric interpolated breath-hold examination; MR: magnetic resonance.  
\*b values for DWI: 0, 1000, and 2000 mm<sup>2</sup>/s.

Prostate gland mpMRI, which is still being updated, aims to distinguish PCa using a combination of several MR sequences. The combination of T2WI, diffusion-weighted imaging (DWI), and dynamic contrast-enhanced imaging (DCEI) provides a systematic method of conducting decision-making processes and a focus on biopsy staging in a more objective manner. However, the information obtained is open to the subjective evaluation of the radiologist who determines the relative possibilities of a differential diagnosis. For this reason, more objective criteria are needed in the evaluation of diagnostic alternatives. To distinguish PCa from prostatitis using mpMRI, the criteria used must be both measurable and consistent. In recent years, apparent diffusion coefficient (ADC) measurements have distinguished between prostatitis and PCa [3]. Esen et al. [7] examined the ability of lower b values to discriminate PCa and prostatitis and showed that increased b values result in decreased sensitivity and increased specificity in the differentiation of PCa from prostatitis.

The aim of the present study was to compare the mpMRI-based measurements obtained from the foci of PCa and prostatitis and to determine the diagnostic performance of MR sequences and the combination of sequences used to differentiate these two disorders.

## Materials and Methods

### Subjects

The institutional review board of Ankara University School of Medicine approved this retrospective, single-center study protocol and waived informed consent.

One hundred consecutive patients who underwent 3.0 Tesla prostate mpMRI between October 2011 and August 2015 and had a prostate biopsy after MR examination were enrolled in the study. Patients were referred to MR examination due to an elevated PSA level, a family history of PCa, or a suspicion of PCa at physical examination. Inclusion criteria were: (1) presence of high image quality prostate MR imaging before biopsy, (2) existence of biopsy-proven prostatitis or PCa, and (3) no history of previous treatment administered to the pelvis. Unenhanced images of three patients with a history of an allergy to contrast material were also included in the study. Twelve patients with both prostatitis and PCa confirmed by pathology, eight patients with suboptimal MR images (extensive artifacts due to motion or rectal gas), and three patients with a history of previous prostate surgery or pelvis radiotherapy were excluded from the study. Of 100 patients, 77 patients with 81 biopsy-proven lesions (44 prostatitis (mean age 65±8 years) and 37 PCa (mean age 63±7 years)) met the inclusion criteria and were enrolled in our study.

### MR Imaging

Before prostate biopsy, MR images were obtained using a 3.0 Tesla system (Verio; Siemens Medical Solutions, Erlangen, Germany). A standard body matrix coil was utilized for signal reception. The multiparametric detection and localization examination consisted of T1-weighted (T1W) images, high-resolution (HR) T2WI, DWI, and DCEI. In the present study, the sequences and planes reviewed were as follows: HR T2W sagittal, coronal, and axial turbo spin-

echo (TSE) images; DWI with three different b values (0, 1000 and 2000 mm<sup>2</sup>/s) obtained in the axial plane using a single-shot multi-slice echo-planar imaging sequence with spectral adiabatic inversion recovery fat suppression; ADC maps, which were automatically generated using a monoexponential decay model including all three b values using Siemens Software Version syngo MR B17; and DCEI images. Before the injection of contrast material, an axial three-dimensional (3D) T1W gradient-echo (GRE) sequence was used to allow the calculation of relative gadolinium chelate concentration curves. During intravenous administration of 0.2 mL/kg of gadolinium chelate at an injection rate of 2.5 mL/s, followed by a 15 mL saline flush, dynamic images were acquired in the axial plane with a 3D fat-suppressed GRE T1W sequence. With this sequence, the entire prostatic volume was repeatedly imaged every 7 s, with the same positioning angle and center as the axial T2W sequence. Then, contrast-enhanced fat-suppressed T1W TSE oblique axial and oblique coronal images were acquired. Table 1 shows the pulse sequence parameters utilized in our study.

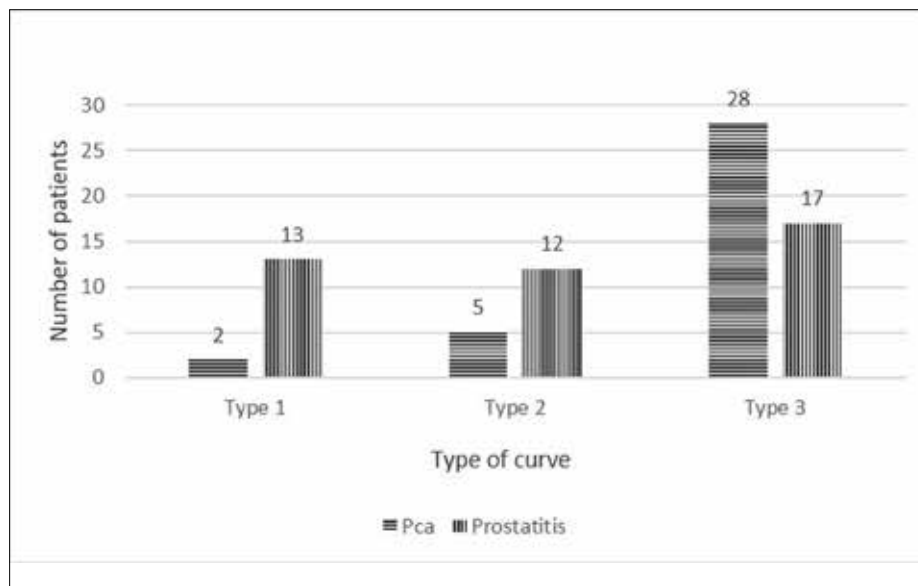
### MRI Analysis

Diagnostic MR images were analyzed using Workstation (Leonardo; Siemens Medical Solutions, Erlangen, Germany) from which DCEI parameters were calculated. Images of all patients were reviewed by three radiologists with 10 years (E.P. and D.S.) and 2 years (H.E.A.) of experience in prostate MRI who were blinded to the clinical history and histology results. Since this was a retrospective study, biopsy results

**Table 2.** Patient and MR imaging characteristics and mean±standard deviation of the measurements of normal tissue, prostate cancer, and prostatitis

	PCA	Prostatitis	Normal	PCA vs. normal (p)	Prostatitis vs. normal (p)	PCA vs. prostatitis (p)
Mean age (years)	65±8 (40-84)	63±7 (47-82)	N/A	N/A	N/A	0.141
Mean PSA (ng/mL)	10.3±7.6 (3.2-37.8)	8.6±6.6 (3.5-41.4)	N/A	N/A	N/A	0.196
Mean prostate volume (mL)	43.6±21 (15-105)	65.1±33 (20-184)	N/A	N/A	N/A	<0.001*
Mean PSA/prostate volume (ng/mL <sup>2</sup> )	0.29±0.3 (0-1.69)	0.16±0.3 (0-2.07)	N/A	N/A	N/A	0.003*
Mean time between the initial diagnostic MR examination and biopsy (days)	3±1.5 (0-5)	3±1.5 (0-5)	N/A	N/A	N/A	N/A
nT2WI	3.2±0.9 (1.91-6.94)	3.8±0.9 (2.6-6.6)	6.6±1.7 (3.19-11.53)	<0.001*	<0.001*	0.003*
ADC value	0.685±128 (0.433-0.980)	0.874±159 (0.561-1.176)	1.173±144 (0.899-1.459)	<0.001*	<0.001*	<0.001*
SI at DWI (b=1000 mm <sup>2</sup> /s)	46±13 (19-79)	40±10 (16-62)	40±7 (24-53)	0.012*	0.435	0.052
SI at DWI (b=2000 mm <sup>2</sup> /s)	29±9 (16-55)	23±5 (13-33)	19±2 (13-25)	<0.001*	<0.001*	0.014*
Peak SI at the dynamic curves	390±96 (235-669)	398±120 (200-763)	244±77 (99-397)	<0.001*	<0.001*	0.862
SI at the end of the dynamic curves	347±78 (208-583)	370±125 (113-763)	274±78 (129-480)	<0.001*	<0.001*	0.388
Mean peak time (s)	141 (37-287)	162 (77-357)	N/A	N/A	N/A	0.137
Mean enhancement percentage	267 (89-498)	243 (70-432)	N/A	N/A	N/A	0.336
Washout percentage	12 (-2-64)	4 (-1-17)	N/A	N/A	N/A	0.003*

-Data are in means.  
Numbers in parentheses indicate minimum and maximum values.  
PCA: prostate cancer; SI: signal intensity; nT2WI: normalized T2-weighted imaging; DWI: diffusion-weighted imaging; N/A: not applicable; MR: magnetic resonance; PSA: prostate-specific antigen; ADC: apparent diffusion coefficient.  
\*Statistically significant results. ADC values: ×10<sup>-3</sup> mm<sup>2</sup>/s.

**Figure 1.** Graph of the frequency of curve types with a cut-off value of 3.15%, according to lesion. Pca: prostate cancer

were correlated with MR images to determine the site of normal tissue, PCa, and prostatitis. For this purpose, one of the authors (A.E.) searched the biopsy results and defined and tabulated the location of the prostate lesion in each patient; however, she did not give any information to the reviewers about the nature of the lesion. She also retrieved data regarding the PSA levels of the patients from the hospital information system.

Initially, prostate volumes were measured and recorded by the reviewers, and PSA/prostate volumes were calculated. The MRI criteria used for the assessment of Prostate Imaging, Reporting and Data System, version 2 (PIRADSv2), as well as signal intensity (SI) on DWI, were evaluated in the present study. After localization of the lesion on MRI, SIs were measured three times on T2WIs and DWIs (b=1000 and b=2000 mm<sup>2</sup>/s, respectively), and the mean values were recorded. SIs of the obturator externus muscle on T2WIs are

**Table 3.** Diagnostic performance of SI values on T2W images, DWI, ADC values, DCEI, and combinations of SI on T2W images, SI on DWI, ADC values, and washout percentage obtained from DCEI for PCa

	Cut-off value	Sensitivity (95% CI)	Specificity (95% CI)	AUC (95% CI)	False negative	PPV (95% CI)	NPV(95% CI)
rT2SI	3.06	56.7% (39-72)	78.5% (63-89)	0.69 (0.57-0.81)	33%	70% (55-81)	67.3% (57-75)
ADC	778	80.5% (64-92)	75% (60-87)	0.82 (0.73-0.91)	18%	72.5% (60-81)	82.5% (70-90)
DWI (b=2000)	29.1	45.7% (28-63)	88% (74-96)	0.68 (0.56-0.80)	34%	76.1% (56-88)	66% (58-72)
Washout percentage	3.15%	80% (63-91)	59.5% (43-74)	0.69 (0.57-0.81)	22%	62.2% (52-71)	78.1% (63-87)
*rT2SI-ADC combined	3.06-778	48.6% (31-65)	88.6% (75-96)	0.68 (0.56-0.80)	33%	78.2% (59-89)	67.2% (59-74)
*ADC-washout percentage combined	778%-3.15% (type 3 curve)	61.7% (43-78)	83.3% (68-93)	0.72 (0.60-0.84)	27%	75% (59-86)	72.9% (63-80)
*rT2SI-washout percentage combined	3.06%-3.15% (type 3 curve)	41.6% (25-59)	90.4% (77-97)	0.66 (0.53-0.79)	36%	78.9% (57-91)	64.4% (57-70)
*SI-DWI (b=2000) and washout percentage combined	29.1%-3.15% (type 3 curve)	42.4% (25-60)	95% (83-99)	0.68 (0.56-0.81)	34%	87.5% (63-96)	66.6% (59-73)
*rT2SI (b=2000) combined	3.06-29.1	22.8% (10-40)	97.6% (87-99)	0.60 (0.47-0.74)	39%	88.8% (51-98)	60.8% (56-65)
*ADC-DWI (b=2000) combined	778-29.1	41.1% (24-59)	97.6% (87-99)	0.69 (0.57-0.81)	33%	93.3% (65-99)	67.2% (60-73)
*rT2SI-ADC-washout percentage combined	3.06%-778%-3.15% (type 3 curve)	77.7% (60-89)	85.7% (71-94)	0.81 (0.71-0.91)	18%	82.3% (68-90)	81.8% (70-89)
*SI-DWI (b=2000), rT2SI, ADC combined	29.1-3.06-778	70.2% (53-84)	88.6% (75-96)	0.78 (0.67-0.89)	22%	83.8% (68-92)	78% (68-85)

Numbers in parentheses indicate 95% CI.  
 PCa: prostate cancer; SI: signal intensity; rT2SI: relative T2-signal intensity; ADC: apparent diffusion coefficient; DWI: diffusion-weighted imaging; DCEI: dynamic contrast-enhanced imaging; AUC: area under the curve; PPV: positive predictive value; NPV: negative predictive value; CI: confidence interval; T2W: T2-weighted.  
 \*All criteria should be positive for prostate cancer diagnosis.  
 \*Combined two criteria were accepted enough for prostate cancer diagnosis. ADC values:  $\times 10^{-3} \text{ mm}^2/\text{s}$ .

also measured. Normalized T2SIs (nT2SIs) are calculated by dividing SIs of the prostate tissue to the SIs of the muscle. The SI time curves obtained from DCEI were analyzed as follows: (1) SI at the initial phase, (2) time and SI values at maximum enhancement, and (3) SI at the end of the curve. The three types of enhancement kinetic curves were assessed as follows: type 1 (progressive enhancement pattern), type 2 (plateau pattern), and type 3 (washout pattern) [8]. A continuous SI increase within the first 3 min was defined as a type 1 curve. The washout percentage was calculated using the following formula:  $(\text{peak SI} - \text{SI at the end of the examination}) / \text{peak SI} \times 100$ . Lesions with a washout percentage of  $>3.15\%$  (cut-off value determined from receiver operating characteristic (ROC) curve analyses) were classified as a type 3 curve; others were accepted as having a plateau pattern and classified as a type 2 curve. The contrast enhancement percentage was calculated using the following formula:  $(\text{peak SI} - \text{SI at the beginning of the examination}) / \text{SI at the beginning of the examination} \times 100$ . Regions of interest were defined by tracing a line free-hand around the perceived tumor margins. Since the objectives of the present study did not include the staging of PCa, scoring according to the PIRADS was not performed.

The mean values of each parameter were compared. The sensitivity, specificity, positive pre-

dictive value (PPV), negative predictive value (NPV), and false-negative rate of significantly different parameters of the two groups (nT2SI, DWI (b=2000  $\text{mm}^2/\text{s}$ ), ADC values, washout percentage) and their combinations in differentiating prostatitis and PCa were determined. Combinations of these statistically significant parameters were classified as follows: (1) all criteria should be positive for PCa diagnosis, (2) two combined criteria were acceptable for PCa diagnosis, and (3) three combined criteria were acceptable for PCa. ROC curves were generated, and area under the curve (AUC) was used to determine how nT2SIs and SI on DWIs (b=2000  $\text{mm}^2/\text{s}$ ), ADC values, and washout percentages operated as discriminatory tests to distinguish prostatitis and PCa. The cut-off values for each of these parameters were determined.

### Biopsy

After MRI (maximum 2 weeks later), core biopsies were obtained from 12 sections of the prostate gland (four quadrants each at the base, mid-gland, and apex), as well as from the target lesion suspected on MRI.

### Statistical Analysis

The results are expressed as mean  $\pm$  standard deviation for continuous variables. Age followed a normal distribution, and groups (PCa vs. prostatitis) were compared using Student's t-test.

PSA value, prostate volume, and PSA/prostate volume followed non-normal distributions, and comparisons between the two groups (PCa vs. prostatitis) were performed using Mann-Whitney U test. Among the MRI data, for the comparison of normal and PCa tissue in the PCa group, normally distributed values (nT2SI, SI on DWI b=1000  $\text{mm}^2/\text{s}$ , and SI at the end of the dynamic curves) were compared using paired t-test, and non-normally distributed values (ADC values, SI on DWI b=2000  $\text{mm}^2/\text{s}$ , and peak SI at the dynamic curves) were compared using Wilcoxon test. In the prostatitis group, for the comparison of normal and prostatitis tissue, normally distributed values (nT2SI and ADC values) were compared using paired t-test, and non-normally distributed values (SI on DWI b=1000  $\text{mm}^2/\text{s}$  and b=2000  $\text{mm}^2/\text{s}$ , peak SI at the dynamic curves, and SI at the end of the dynamic curves) were compared using Wilcoxon test. For comparisons between the PCa and prostatitis groups, normally distributed nT2SI and ADC values were compared using Student's t-test. Non-normally distributed SI on DWI b=1000  $\text{mm}^2/\text{s}$  and b=2000  $\text{mm}^2/\text{s}$ , peak SI at the dynamic curves, and SI at the end of the dynamic curves were compared using Wilcoxon test. The sensitivity, specificity, PPV, NPV, and false-negative rate of significantly different parameters of the two groups (nT2SI, SI on DWI

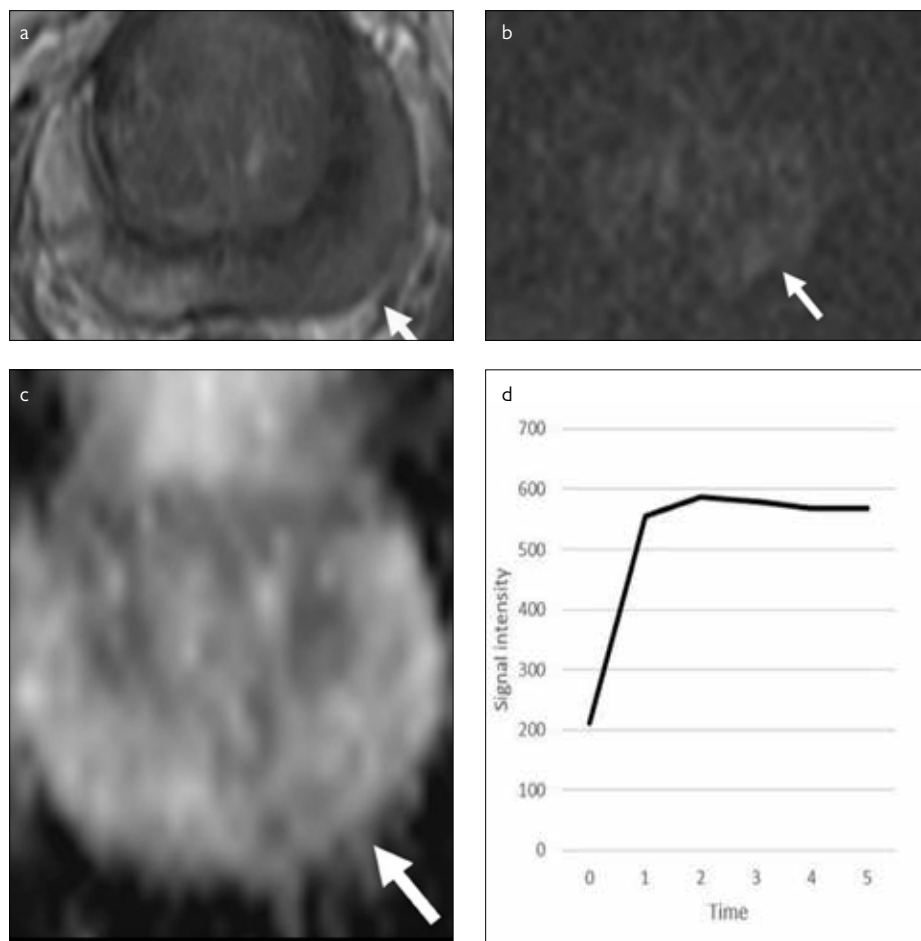


**Figure 2. a-d.** Biopsy-proven prostatitis. Axial T2-weighted imaging (a), diffusion-weighted imaging ( $b=2000 \text{ mm}^2/\text{s}$ ) (b), ADC map (c), and signal intensity/time curve derived from dynamic-enhanced images (d) show a capsule-contained left peripheral T2 hypointense lesion (a), which is hyperintense on diffusion-weighted imaging (b). The ADC value in the region of the lesion (arrow) is  $1.065 \times 10^{-3} \text{ mm}^2/\text{s}$  (c) and shows type 2 curve, with a plateau pattern (d).

( $b=2000 \text{ mm}^2/\text{s}$ ), ADC values, and washout percentage) and their combinations in differentiating prostatitis and PCa were determined. ROC curves were generated, and AUC was used to determine how nT2SI and SIs on DWIs ( $b=2000 \text{ mm}^2/\text{s}$ ), ADC values, and washout percentages and their combinations operated as discriminatory tests to distinguish prostatitis and PCa. The cut-off values for each of these parameters were determined. The frequency of curve types was compared using chi-square test.

Data analysis was made using the Statistical Package for the Social Sciences (SPSS Inc.; Chicago, IL, USA) 11.5 and MedCalc software (MedCalc, version 16; Mariakerke, Belgium). Biopsy results were accepted as the standard of reference. A  $p < 0.05$  was considered as significant.

## Results

A total of 77 patients with biopsy-proven prostatitis or PCa between October 2011 and August 2015 were included in the study. Four patients had two lesions. There were 37 can-

cer-positive and 44 prostatitis-positive biopsy specimens. Table 2 shows the characteristics of the prostatitis and PCa groups. Age and PSA levels were not significantly different between the prostatitis and PCa groups ( $p=0.196$ ). The mean prostate volume ( $65.1 \text{ mL}$  vs.  $43.6 \text{ mL}$ ,  $p < 0.001$ ) and mean PSA/prostate volume ( $0.29$  vs.  $0.16$ ,  $p=0.003$ ) were significantly higher in the PCa group than in the prostatitis group.

Table 2 shows the MRI characteristics of normal tissue, PCa, and prostatitis. The mean nT2SIs ( $6.6 \pm 1.7$  vs.  $3.2 \pm 0.9$  vs.  $3.8 \pm 0.9$ ) and DWIs ( $b=2000 \text{ mm}^2/\text{s}$ ) (29 vs. 23 vs. 19) and the mean ADC values ( $0.685 \times 10^{-3} \text{ mm}^2/\text{s}$  vs.  $0.874 \times 10^{-3} \text{ mm}^2/\text{s}$  vs.  $1.173 \times 10^{-3} \text{ mm}^2/\text{s}$ ) were significantly different among the PCa, prostatitis, and normal groups ( $p < 0.05$ ) (Table 2). Compared with the normal tissue group, both the PCa and the prostatitis groups showed significantly lower nT2SI ( $p < 0.001$  and  $p < 0.001$ ), as well as lower ADC values ( $p < 0.001$  and  $p < 0.001$ ) and significantly higher SI on DWI ( $b=2000 \text{ mm}^2/\text{s}$ ) ( $p < 0.001$  and  $p < 0.001$ ); the values obtained in the PCa

group were significantly higher than those obtained in the prostatitis group ( $p=0.014$ ) (Table 2). The mean SI on DWI  $b=1000 \text{ mm}^2/\text{s}$  was significantly higher in the PCa group than in the normal tissue group ( $46$  vs.  $40$ ,  $p=0.012$ ) but was similar between the prostatitis and PCa groups ( $40$  vs.  $46$ ,  $p=0.052$ ) and the prostatitis and normal tissue groups ( $40$  vs.  $40$ ,  $p=0.435$ ) (Table 2). After contrast medium injection, both peak SI ( $390$  vs.  $398$  vs.  $244$ ) and SI at the end of the examination ( $347$  vs.  $370$  vs.  $274$ ) were significantly higher in the PCa and prostatitis groups than in the normal tissue group ( $p < 0.001$ ,  $p < 0.001$ ,  $p < 0.001$ , and  $p < 0.001$ ) (Table 2). However, there was no significant difference between the PCa and prostatitis groups in terms of peak SI ( $390$  vs.  $398$ ,  $p=0.862$ ), SI at the end of the examination ( $347$  vs.  $370$ ,  $p=0.388$ ), and peak time ( $141$  vs.  $162 \text{ s}$ ,  $p=0.137$ ) (Table 2). The prostatitis and PCa groups showed similar contrast enhancement ( $p=0.336$ ) (Table 2), but the contrast washout percentage was significantly higher in the PCa group than in the prostatitis group ( $12$  vs.  $4$ ,  $p=0.003$ ), with a cut-off value of 3.15% and AUC of 0.69 (95% CI: 0.57-0.81) (Table 3).

The ROC curves of the nT2SIs, ADC values, SI on DWI ( $b=2000 \text{ mm}^2/\text{s}$ ), and washout percentage yielded AUCs of 0.69, 0.82, 0.68, and 0.69, respectively (Table 3). Among all the criteria, the mean ADC values showed both high sensitivity (80.5%, 95% CI: 64-92) and specificity (75%, 95% CI: 60-87) in addition to low false-negative rates (18%) (Table 3). The cut-off values for each of the parameters are listed in Table 3.

The ADC values demonstrated a moderate positive correlation with nT2SI ( $r=0.404$ ,  $p=0.000$ ), a moderate negative correlation with SI on DWI ( $b=2000 \text{ mm}^2/\text{s}$ ) ( $r=-0.403$ ,  $p=0.000$ ), and a weak negative correlation with washout percentage ( $r=-0.332$ ,  $p=0.003$ ). The washout percentage showed a weak positive correlation with SI on DWI ( $b=2000 \text{ mm}^2/\text{s}$ ) ( $r=0.325$ ,  $p=0.005$ ).

A type 1 curve was significantly more frequent in prostatitis cases than in PCa cases ( $p=0.011$ ) (Figure 1), whereas a type 3 curve was more frequently observed in PCa than in prostatitis (Figure 1). The frequencies of curve types, determined by a cut-off value of 3.15% (cut-off value determined from ROC curve analyses) according to the lesion, are summarized in Figure 1. The AUC was calculated as 0.69 (95% CI: 0.57-0.81,  $p=0.003$ ) when the washout percentage was 3.15%, and a type 3 curve was accepted as favoring PCa.



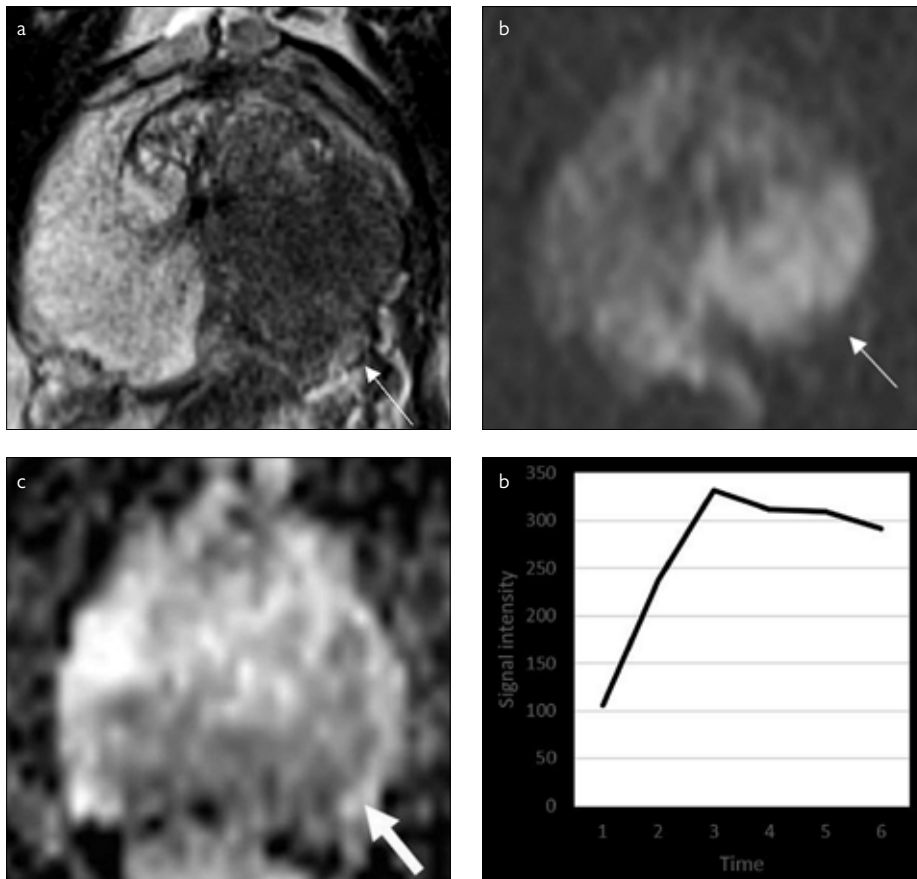


**Figure 3. a-d.** Biopsy-proven prostate cancer. Axial T2-weighted imaging (a), diffusion-weighted imaging ( $b=2000 \text{ mm}^2/\text{s}$ ) (b), ADC map (c), and signal intensity/time curve derived from dynamic-enhanced images (d) show a left-sided peripheral zone lesion (arrow) with extracapsular invasion on T2-weighted imaging (a), which has increased signal intensity on diffusion-weighted imaging (arrow) (b). ADC map of the lesion (arrow) shows lower signal, indicating restricted diffusion (c). Signal intensity/time curve derived from dynamic-enhanced images shows type 3 curve, with washout pattern (d).

By using the cut-off values for discriminating patients with PCa, the diagnostic performance of the combinations of four criteria (nT2SI, ADC, DWI at  $b=2000 \text{ mm}^2/\text{s}$ , and washout percentage) was calculated (Table 3). The combination of nT2SI, ADC value, and washout percentage (positivity in two out of the three criteria was accepted as sufficient for a diagnosis of PCa) yielded both higher sensitivity and specificity, as well as the highest AUC (0.81, 95% CI: 0.71-0.91) (Table 3). MR images of biopsy-proven prostatitis and PCa are shown in Figures 2 and 3, respectively.

## Discussion

The ability to accurately differentiate prostatitis from PCa is critical to manage patients and avoid unnecessary treatment. As shown in our study, increased prostate and PSA/prostate volumes were clinical indicators of prostatitis and PCa. However, imaging is generally needed for differential diagnosis. When examining studies of PCa, data regarding the differentiation between PCa and prostatitis are limited [2, 3].

Our results highlight several important issues and difficulties with regard to the discrimination of prostatitis from PCa using MRI. T2WIs are generally used for the evaluation of the prostate. However, as mentioned above, the specificity of T2WI is low [2, 9].

The evidence presented in the presented study suggests that both PCa and prostatitis can be distinguished from normal tissue using the ADC values, nT2SI, and SI on DWI ( $b=2000 \text{ mm}^2/\text{s}$ ). However, prostatitis cannot be discriminated from normal tissue by an SI of  $b=1000 \text{ mm}^2/\text{s}$ . As previously indicated, diffusion values lower than  $b=1400 \text{ mm}^2/\text{s}$  are not recommended in prostate imaging [9].

In the present study, four parameters were examined to distinguish between prostatitis and PCa. These parameters included nT2SI, SIs on DWI ( $b=2000 \text{ mm}^2/\text{s}$ ), ADC values, and washout percentage. Among these four criteria, the ADC values showed the highest AUC, high sensitivity and specificity, and low false-negative

rates. The ADC values also showed a positive correlation with nT2SI and a negative correlation with SI on DWI ( $b=2000 \text{ mm}^2/\text{s}$ ) and washout percentage, as expected.

Compared with prostatitis, PCa showed higher SI on DWI ( $b=2000 \text{ mm}^2/\text{s}$ ), lower nT2SI, and lower ADC values. Moreover, the washout percentage of PCa was higher than that of prostatitis.

The diagnostic accuracy of ADC measurements appears to be higher than that of T2WI, which is standard in prostate imaging. The higher cellularity of PCa over prostatitis is reflected by lower ADC values ( $0.685 \times 10^{-3} \text{ mm}^2/\text{s}$  vs.  $0.874 \times 10^{-3} \text{ mm}^2/\text{s}$ ) and higher SI on DWI  $b=2000 \text{ mm}^2/\text{s}$  (29 vs. 23). Diffusion parameters (ADC value and SI on DWI  $b=2000 \text{ mm}^2/\text{s}$ ) yielded the highest PPV among all the single and combined criteria.

Overlap of the enhancement characteristics between PCa and benign prostatic hypertrophy has been previously described [10-12]. PCa is known to exhibit variable contrast kinetics [2]. Moreover, some malignant tumors show early washout, and some continue to enhance progressively [2]. In the 2015 version of PIRADS, this potential diagnostic limitation of DCEI was emphasized [9], and we made a similar observation. Quantitative DCEI parameters, such as time to peak and mean enhancement percentage, were not distinguishing factors between PCa and prostatitis. In our study, compared with prostatitis, PCa often demonstrated early enhancement; however, there was no significant difference in peak time, which may be due to the heterogeneity of the PCa group demonstrated by both low- and high-grade tumors. However, the washout percentage appeared to be a better discriminator of PCa (AUC: 0.69, 95% CI: 0.57-0.81).

It remains unclear which criteria can be used to determine the curve type [9]. Based on the results of our study, we suggest that lesions with any of the curve types other than the type 1 curve should raise suspicion of PCa. When a washout percentage of 3.15% and a type 3 curve are accepted as favoring PCa, PCa can be distinguished from prostatitis.

The differentiation of PCa from prostatitis remains a problem characterized by low sensitivity and specificity values. For this reason, in the present study, we sought to increase the diagnostic efficiency by combining different criteria. When all evaluated criteria were expected to be positive, all criteria added to the ADC values reduced the sensitivity of the ADC and increased the

false-negative rates. If two out of the three criteria were positive, they were accepted as sufficient for the diagnosis of PCa. The combination of nT2SI, ADC values, and washout percentage (cut-off value 3.15% and type 3 curve) increased the specificity of the ADC values and reduced the false-negative rate. In addition, the adoption of all curves other than the type 1 curve in favor of PCa alone was sufficient for high sensitivity. Furthermore, the combination of this finding with nT2SI and ADC values did not change the sensitivity and specificity, and the combination of all highlighted criteria (nT2SI, SI on DWI at  $b=2000$  mm<sup>2</sup>/s, ADC values, and washout percentage) did not markedly improve the sensitivity of ADC and reduced the specificity. Combinations with DWI ( $b=2000$  mm<sup>2</sup>/s) did not increase the sensitivity of nT2SIs, ADC values, or the washout percentage but increased the false-negative rates.

Despite a consensus indicating diffusion restriction, there was substantial variation in the reported ADCs of PCa [3]. As our study results demonstrated, the average ADCs differed significantly between normal tissue, PCa, and prostatitis ( $1.17 \times 10^{-3}$  mm<sup>2</sup>/s vs.  $0.68 \times 10^{-3}$  mm<sup>2</sup>/s vs.  $0.87 \times 10^{-3}$  mm<sup>2</sup>/s, respectively,  $p=0.000$ ); similar differences in the average ADC were reported by Nagel et al. [3] ( $1.22 \times 10^{-3}$  mm<sup>2</sup>/s vs.  $0.88 \times 10^{-3}$  mm<sup>2</sup>/s vs.  $1.08 \times 10^{-3}$  mm<sup>2</sup>/s, respectively). In contrast to our study, the study by Esen et al. [7] did not show significant differences between the mean ADC values of normal tissue and prostatitis at b values of 100, 600, and 1000 mm<sup>2</sup>/s. This result may be due to relatively lower b values selected in their study; thus, emphasis should be placed on the importance of using higher b values in prostate imaging.

Our study had several limitations. First, this was a retrospective study with a relatively small sample size. Second, the lack of classification of pathology specimens as low-grade and high-grade PCa is another limitation. Finally, most importantly, there was a potential for incorrect estimation of biopsy-proven lesions on MRI because the biopsy was not MR guided.

In conclusion, mpMRI of the prostate gland at 3.0 Tesla enabled differentiation between normal tissue, PCa, and prostatitis. nT2SI, SI on DWI ( $b=2000$  mm<sup>2</sup>/s), ADC values, and washout percentage were identified as MRI criteria for discriminating PCa from prostatitis. Compared with all of the single and most of the combined criteria, the ADC values alone demonstrated higher sensitivity and specificity. Moreover, the combination of nT2SI, ADC values, and washout percentage (at least two positive criteria were sufficient for a diagnosis of PCa) yielded the highest sensitivity and specificity among all combinations. The use of anatomic and functional MRI sequences revealed a difference between prostatitis and PCa. However, caution should be exercised when interpreting these results, and the weaknesses of each sequence should be realized and taken into consideration when making decisions regarding the results.

**Ethics Committee Approval:** Ethics committee approval was received for this study from the ethics committee of Ankara University School of Medicine.

**Informed Consent:** Informed consent was waived by the Ethics Committee.

**Peer-review:** Externally peer-reviewed.

**Author Contributions:** Concept – E.P., A.E.; Design – E.P., A.E.; Supervision – A.E., M.I.E., Resource – A.E., M.I.E.; Materials – E.P., A.E.; Data Collection and/or Processing – E.P., S.H., D.Y.S.; Analysis and /or Interpretation – E.P.; Literature Search – E.P.; Writing – E.P., A.E.; Critical Reviews – A.E., M.I.E.

**Conflict of Interest:** The authors have no conflicts of interest to declare.

**Financial Disclosure:** The authors declared that this study has received no financial support.

## References

1. Krieger JN, Lee SWH, Jeon J, Cheah PY, Liong ML, Riley DE. Epidemiology of prostatitis. *Int J Antimicrob Agents* 2008; 31: 85-90. [\[CrossRef\]](#)
2. Sah VK, Wang L, Min X, et al. Multiparametric MR imaging in diagnosis of chronic prostatitis and

its differentiation from prostate cancer. *Radiol Infectious Diseases*. 2015; 1: 70-77. [\[CrossRef\]](#)

3. Nagel KN, Schouten MG, Hambrock T, et al. Differentiation of prostatitis and prostate cancer by using diffusion-weighted MR imaging and MR-guided biopsy at 3 T. *Radiology* 2013; 267: 164-72. [\[CrossRef\]](#)
4. Bonekamp D, Jacobs MA, El-Khouli R, Stoianovici D, Macura KJ. Advancements in MR imaging of the prostate: from diagnosis to interventions. *Radiographics* 2011; 31: 677-703. [\[CrossRef\]](#)
5. Kitzing YX, Prando A, Varol C, Karczmar GS, Maclean F, Oto A. Benign conditions that mimic prostate carcinoma: MR imaging features with histopathologic correlation. *Radiographics* 2016; 36: 162-175. [\[CrossRef\]](#)
6. Langer DL, van der Kwast TH, Evans AJ, Trachtenberg J, Wilson BC, Haider MA. Prostate cancer detection with multi-parametric MRI: logistic regression analysis of quantitative T2, diffusion-weighted imaging, and dynamic contrast-enhanced MRI. *J Magn Reson Imaging* 2009; 30: 327-334. [\[CrossRef\]](#)
7. Esen M, Onur MR, Akpolat N, Orhan I, Kocakoc E. Utility of ADC measurement on diffusion-weighted MRI in differentiation of prostate cancer, normal prostate and prostatitis. *Quant Imaging Med Surg* 2013; 3: 210-215.
8. Bluemke DA, Gatsonis CA, Chen MH, et al. Magnetic resonance imaging of the breast prior to biopsy. *JAMA* 2004; 292: 2735-2742. [\[CrossRef\]](#)
9. Weinreb JC, Barentsz JO, Choyke PL, et al. PI-RADS Prostate Imaging-Reporting and Data System: 2015, Version 2. *Eur Urol* 2016; 69: 16-40. [\[CrossRef\]](#)
10. Oto A, Kayhan A, Jiang Y, et al. Prostate cancer: differentiation of central gland cancer from benign prostatic hyperplasia by using diffusion-weighted and dynamic contrast-enhanced MR imaging. *Radiology* 2010; 257: 715-723. [\[CrossRef\]](#)
11. Padhani AR, Gapinski CJ, Macvicar DA, et al. Dynamic contrast enhanced MRI of prostate cancer: correlation with morphology and tumour stage, histological grade and PSA. *Clin Radiol* 2000; 55: 99-109. [\[CrossRef\]](#)
12. Deering RE, Bigler SA, Brown M, Brawer MK. Microvasculature in benign prostatic hyperplasia. *Prostate* 1995; 26: 111-115. [\[CrossRef\]](#)